

An Explorative Study of Applying Reichardt-Model in Visual Servo Control

Haiyan Wu¹, Tianguang Zhang¹, Alexander Borst²,
Kolja Kühnlenz¹ and Martin Buss¹

¹Institute of Automatic Control Engineering (LSR)
Technische Universität München
D-80290 München, Germany

²Department of Systems and Computational Neurobiology
Max Planck Institute of Neurobiology
Am Klopferspitz 18, D-82152 Martinsried, Germany

Email: {tg.zhang, kolja.kuehnlenz, m.buss}@ieee.org,
haiyan.wu@tum.de, borst@neuro.mpg.de

Abstract—In this paper, a biologically inspired motion detector (Reichardt-Model) is introduced into visual servo control to ensure stability of the system with high gain and time-delay in its feedback. As a consequence of the specific velocity dependence of the Reichardt-Model, the stability margin of the visual servo control is increased and high overall gains, thus, better performance are achievable. As the first step of the study, the control performance of visual servo control with different sampling and different time-delay in its visual feedback loop, and velocity control performance with Reichardt-Model are investigated. A high-speed visual servo control system with up to 500Hz framerate is built up on a 1-DOF linear axis. With the results of simulation, the inner velocity control loop with Reichardt-Model is demonstrated to be more stable than standard model without Reichardt-Model when feedback gain increases and time-delay is presented. The results of real-time experiments show an improved performance by utilizing high-speed visual feedback or when the overall time-delay is small.

I. INTRODUCTION

An important aspect in the research field of robotics and automation is the use of high-speed visual servo control loops running at framerate of several 100Hz controlling and stabilizing the motion of the system. How to improve the control performance and to ensure the stability of visual servo control despite the presence of time-delay is an important issue.

Visual servo is the fusion of results from many elemental areas including real-time image processing, kinematics, dynamics, control theory, and real-time computing [1]. However, in most of the previous robot systems, the processing rate of vision sensors, for example, CCD (30Hz) which is typical, is much slower than the servo rate for robot control (1kHz) [2]. The faster a manipulator moves, the greater is the uncertainty. Therefore, the challenge issue here is to achieve high-speed visual feedback as well as high-speed motion in order to perform tasks robustly. Moreover, a suitable controller should be designed to ensure the stability of the system. Several approaches have been carried out recently.

In [3], a regrasping strategy based on visual feedback is presented. A high-speed multi-fingered hand is chosen and a high-speed visual processing is achieved, within 1ms. In [4], an approach named multi-input multi-output (MIMO) predictive control is used to model and control high-speed 6-DOF visual servo control loop. The sampling frequency of the visual loop is 120Hz. In [5], a 1 ms vision system is developed and applied to high-speed target tracking .

Besides, the research in the field of biologics gives the inspiration of building a stable visual servo control system. A fly's (e.g. Calliphora Vicina) vision system comprises several photoreceptors and motion detectors which are specialized for the detection of optical flow fields of typical motion behaviors [6]. The Reichardt-detector [7] and its variants [8][9][10] are well-known motion detector models which are applied to simulate the fly's motion detection system. It has been demonstrated in [11] that, as the sensory input is lagged by a time-delay, the Reichardt-Model in the optomotor system leads to a stable performance at least if it operates with a high gain in its feedback. If the algorithm of fly's motion detection can be executed in visual servo control, it will be more efficient, stable and can fulfill the requirements of real-time applications (e.g., implement the Reichardt-Model on FPGA [12]).

In this paper, a high-speed image-based visual servoing (IBVS) is established on a linear system of 1-DOF. An array of elaborated Reichardt-Model is implemented to calculate the translational velocity of the camera. The control performance of the IBVS with visual feedback of different frequency is presented. Besides, velocity control with and without Reichardt-Model is tested both in simulation and real-time experiment. With the results of simulation, velocity control with Reichardt-Model is demonstrated to be more stable than standard model without Reichardt-Model.

The remainder of this paper is organized as follows: firstly, in Section II, the control problem and control law for visual servo control are presented. In Section III, the basic EMD

and an elaborated EMD model as well as its application in inner velocity control loop of visual servo control are introduced. Simulation results of velocity control are given in Section IV. The experimental setup and experimental results are shown in Section V and conclusions are given in Section VI.

II. IMAGE-BASED VISUAL SERVOING (IBVS)

Position-based visual servoing (PBVS) and IBVS are two traditional ways for vision-based robot control. They are classified according to error information connected to the controller. In PBVS system, the error is computed in the 3D Cartesian space, while in IBVS system the error is directly computed in the 2D image space [13]. Moreover, new visual servo control techniques are proposed: hybrid visual servo control approaches (e.g. 2 1/2D visual servo control in [14] which uses the error part in 3D Cartesian space and part in 2D image space) and motion-based visual servo control (the error is a function of optical flow [15] [16]). In this paper, the IBVS is chosen since it is known to be robust not only with respect to camera but also to robot calibration errors [17].

A. Control Problem

In IBVS, the error information is extracted from image space. The desired image features are denoted as ξ_d in this paper. These features can be obtained by using a "teach-by-showing" strategy [18]: moving the robot to the reference desired position, the features extracted from the corresponding image are defined as ξ_d (e.g., coordinates of the object's center in the image plane). The objective is to control the robot configuration to generate the prescribed desired output ξ_d in the image plane. However, the desired robot configuration is not given. The image error is: $\tilde{\xi} = \xi_d - \xi$. Therefore, the control aim is to ensure that: $\lim_{t \rightarrow \infty} \tilde{\xi} = 0$. Since the convergence is theoretically ensured only in a region around the desired position, the initial feature error should be sufficiently small.

B. Control Law

The following control law proposed in [19] is chosen :

$$\tau = J(q, \xi, Z)^T K_p \tilde{\xi} - K_v \dot{q} + g(q) \quad (1)$$

where

$$J(q, \xi, Z) = J_{image}(\xi, Z) \begin{bmatrix} R_c(q) & 0 \\ 0 & R_c(q) \end{bmatrix} J_g(q) \quad (2)$$

K_p and K_v are the symmetric positive definite proportional and derivative matrices which are chosen by the designer. $R_c(q)$ is the orientation of the camera frame with respect to the robot frame and $J_g(q)$ is the robot geometric Jacobian. In our experiment, the system is of 1-DOF, thus $J(q, \xi, Z)$ is the same as the image Jacobian matrix $J_{image}(\xi, Z)$, defined by:

$$J_{image}(\xi, Z) = \begin{bmatrix} \frac{\alpha\lambda}{Z} & 0 & \frac{x}{Z} & -\frac{xy}{\alpha\lambda} & \frac{\alpha^2\lambda^2+x^2}{\alpha\lambda} & y \\ 0 & \frac{\alpha\lambda}{Z} & -\frac{y}{Z} & -\frac{\alpha^2\lambda^2+y^2}{\alpha\lambda} & \frac{xy}{\alpha\lambda} & -x \end{bmatrix} \quad (3)$$

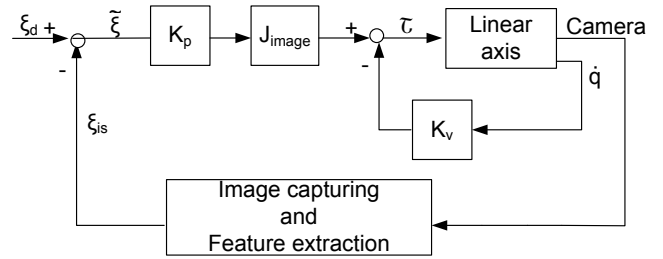


Fig. 1: Block diagram of the IBVS system with position sensor

where $[x \ y]^T$ is the coordinates of the object center in the image plane, α is the scaling factor (in pixels/meter), λ is the focal length. They are intrinsic parameters of the camera. The depth information Z can be obtained either from multi camera, knowledge of the geometric relationship or additional external sensor. The $J_{image}(\xi, Z)$ describes the robot motion in terms of the motion of the feature points. In our 1-DOF system, $J_{image}(\xi, Z) = \frac{\alpha\lambda}{Z}$

III. REICHARDT-MODEL IN IBVS

As introduced in Section II, the feature error $\tilde{\xi}$ in image plane and the joint velocity of the robot are involved in the control law. In the experiment, the joint velocity of the 1-DOF system is the velocity of the end-effector. It can be easily derived from a inside position sensor and the block diagram of the system is given in Fig.1. There are two closed loops in the model working at different frequency: the inner loop for velocity control works at high frequency (e.g.1000Hz), while the outer loop works at relative low frequency (e.g. from 30Hz to 500Hz depending on the frequency of the image processing).

An alternative to the system in Fig.1 is to get the velocity of the end-effector directly from the image plane. Therefore, the position sensor is discarded from the system and only one camera is demanded. Different methods could be applied to calculate the optical flow from image sequence, e.g. SSD algorithm, Lucas&Kanade method, Horn-Schunck method and so on.

However, there is a shortcoming with such a system. By introducing the optical flow calculation into the inner loop, high gain in the velocity control loop, thus, good performance are not achievable due to the time-delay. The time-delay here consists of several parts: camera exposure time, time for image transferring and image processing, time for data distribution (a distributed system is selected in the experiment). To overcome this drawback, a biologically inspired motion detector Reichardt-Model is introduced. As demonstrated in [11], when its overall gain is large (for the sake of better performance: compensate disturbances efficiently), the optomotor system of the fly containing Reichardt-Model in its closed loop does not get unstable, while a standard linear system without Reichardt-Model becomes unstable. This interesting phenomena inspired us to apply the Reichardt-Model in the IBVS. An example

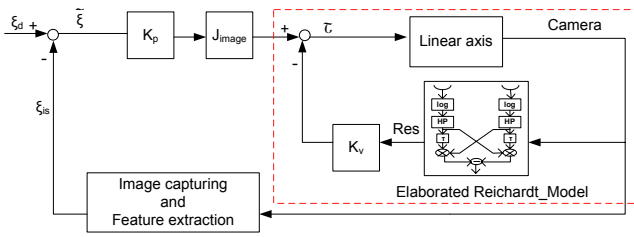


Fig. 2: Block diagram of inner velocity control with Reichardt-Model

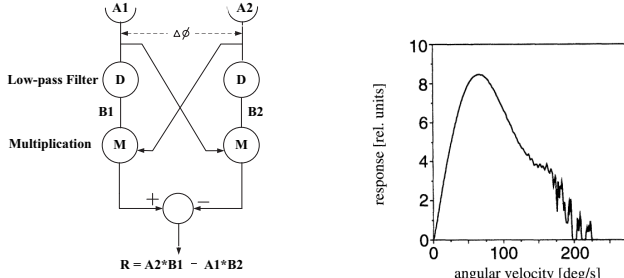


Fig. 3: The simple Reichardt-model [6] and its velocity dependent response [11].

of introducing Reichardt-Model into inner velocity control loop is shown in Fig.2. An array of Reichardt-Model is applied to the image and the responses of each model are summed up which represents the relative velocity of the end-effector with respect to the object. In the following part, the intrinsic properties of the Reichardt-Model and an elaborated Reichardt-Model are introduced.

A. Reichardt-Model

The earliest and probably the most famous model of motion detector inspired by biological systems was developed by Reichardt and Hassentein in 1956 [7]. Fig.3 presents a simplified version of the correlator model.

A1 and A2 are two photoreceptors and they are respectively temporally delayed by the low-pass filter D. With $A1(t)$ and $A2(t)$ representing the input signals at the left and right input channels, and $B1(t)$ and $B2(t)$ representing the corresponding filtered signals, one obtains the output $R(t)$ of a motion detector:

$$R(t) = A2(t) \cdot B1(t) - A1(t) \cdot B2(t). \quad (4)$$

The detector generates a direction sensitive response because of the subtraction between the two symmetric detector halves. The velocity dependence of the response of the Reichardt-Model is shown in Fig.3. The model response first increases with increasing velocity, reaches a maximum and then decreases again. Hence, the gain of the motion detection system in the fly's optomotor pathway is not constant, but becomes small at high velocities [11].

However, the response of the Reichardt detector is not always as simple as a peak. For example, when the input is a pulse, the sign of the response does not directly indicate motion direction [12].

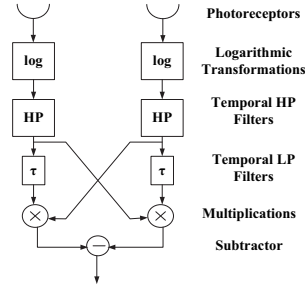


Fig. 4: Elaborated Reichardt-Model

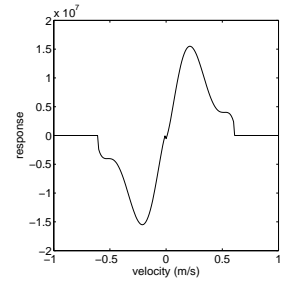


Fig. 5: Response of Reichardt-Model in the experiment.

B. The Elaborated Reichardt-Model

The simple Reichardt detector has two major drawbacks:

- its response is sensitive to edge contrast, reducing robustness to lighting conditions;
- its response to step edges is complicated, making scene interpretation difficult.

Therefore, the simple detector has been improved and two preprocessors are added:

- logarithmic transformation is applied in order to reduce the sensitivity to lighting conditions directly after the receptors;
- this is followed by a temporal high pass filter in order to obtain a simple response to the most common edge type as step edge in natural images.

The elaborated EMD is shown in Fig.4, which is also proposed in [?]. The moving pulse signal (or equivalently a moving step edge) is transformed by the temporal HP filter into a moving peak, and thus, leading to a simple response. The response of this elaborated motion detector is still bell-shaped.

IV. SIMULATION OF VELOCITY CONTROL

In this part, the velocity control model presented in Fig.2 (model in the red dashed line rectangle) is simulated. In the simulation it is assumed that, an object moves at a certain velocity and the goal of the velocity control is to compensate the motion between the end-effector and the object. Therefore, the desired relative velocity of the end-effector V_d is set to zero.

First of all, the response of the Reichardt-Model with respect to velocity is observed. In the experiment, the following parameters are chosen for the Reichardt-Model: $\tau_H = 3.3$, $\tau_L = 2$, $\phi = 1$. Based on sampled examples observed in real-time experiment, the response curve given by Fig.5 is then obtained through interpolation. The response is also bell-shaped which is similar to Fig.3.

In order to compare velocity control performances of models with and without Reichardt-Model, the feedback gains in both models that lead the end-effector motion to 70% of the object velocity are normalized to one (following [11]).

Fig.6 and Fig.7 are the simulation results of the end-effector's velocity and position when the feedback gain is small in both models.

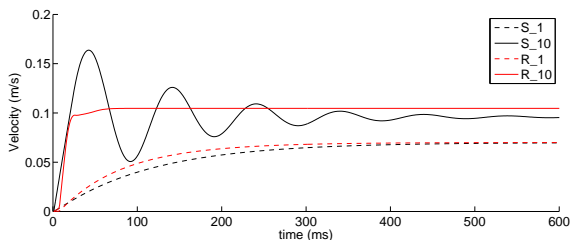


Fig. 6: Velocity of the end-effector in velocity control with/without Reichardt-Model when feedback gain is small.

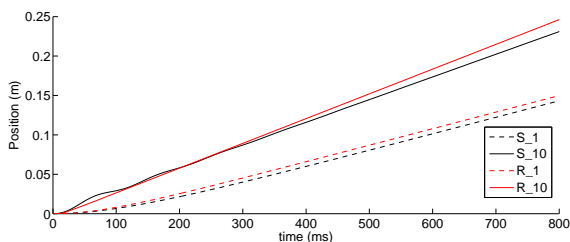


Fig. 7: Position of the end-effector in velocity control with/without Reichardt-Model when feedback gain is small.

The object moves at $0.1m/s$. The curves s_1 and s_{10} are the results of standard model when gain is 1 and 10, while R_1 and R_{10} are the results of model with Reichardt-Model. In this case, both systems settle down in steady state.

However, when the feedback gain increases, the model without Reichardt-Model gets unstable, while model with Reichardt-Model is still in control which oscillates with certain velocity (shown in Fig.8 and Fig.9).

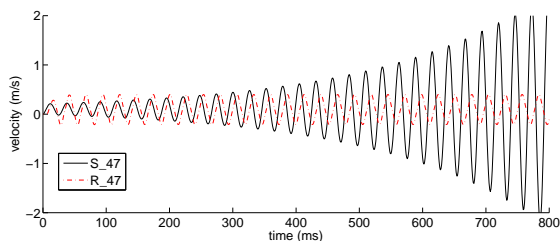


Fig. 8: Velocity of the end-effector in velocity control with/without Reichardt-Model when feedback gain is 47.

The results of the simulation show that, when time-delay is presented and the overall feedback gain gets relative high, inner velocity control loop with Reichardt-Model is more stable than standard model without Reichardt-Model.

V. EXPERIMENTS

Firstly, the velocity control model simulated in Section IV is also tested in real-time experiment. Besides, a simple high-speed IBVS system with position sensor in its inner feedback loop is firstly developed to show the control performance

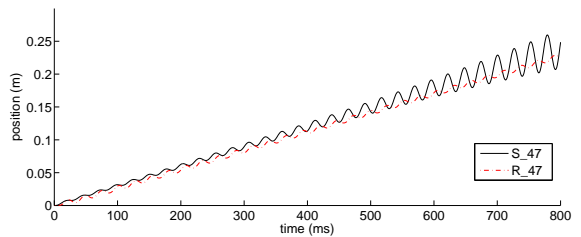


Fig. 9: Position of the end-effector in velocity control with/without Reichardt-Model when feedback gain is 47.

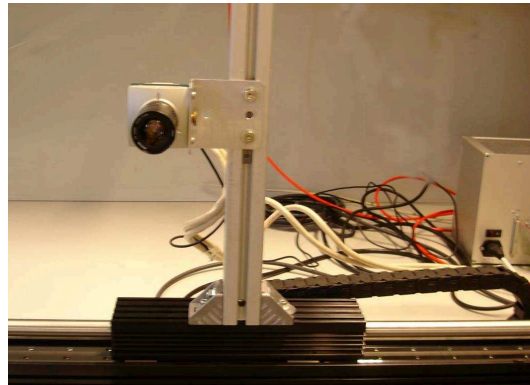


Fig. 10: Experimental Setup

with the visual feedback which provides the feature error in image plane.

A. Experimental Setup

A linear axis (STB-2510 [20]) depicted in Fig.10 is selected as a basic module. Since it is a 1-DOF manipulator, the system is much simplified. Its end-effector is a slide and moves horizontally. The peak velocity that can be achieved is $4.6m/s$. A non-contact position sensor is integrated into the system. Therefore, the velocity of the slide which is required in the control law (eq.1) can be easily computed. The control of the linear axis is through a Simulink program, which runs on a PC (i686, AMD 64 Processor 3000+) with fixed sampling time 1ms.

A high speed CMOS imaging camera (Mikrotron MC1319) is mounted on the slide. It provides high speed imaging with up to 500 full frames per second. The intrinsic camera parameters contains: focal length $\lambda = 17mm$, scaling factor $\alpha = 88,888pixels/m$. The camera configuration is fixed during the experiment. The captured image is transferred to a host PC (x86_64, AMD 64x2 dual core Processor 5200+) through PCIe.

B. Parameter Settings and Experimental Results

Three experiments are carried out. In the first experiment, the velocity control model is tested and the control performance is presented. In the second experiment, the system has constant time-delay but with visual feedback of different sampling rate. In the last experiment, visual feedback is set to have a frequency of 500Hz but with different time-delay.

Experiment1: In this experiment, the model simulated in Section IV is tested on the linear axis. The camera works at the framerate of 30fps and has a resolution of 640×480 pixels. The time for computing optical flow through Reichardt-Model in image plane is about 20ms. The results of velocity control with and without Reichardt-Model in the feedback loop are given by Fig.11 and Fig.12. S_1 and S_50 are the results of the standard model when feedback gain is 1 and 50, while R_1 and R_50 are the results of control with Reichardt-Model.

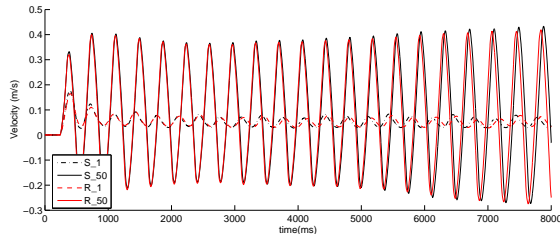


Fig. 11: Velocity of the end-effector in velocity control with/wihtout Reichardt-Model when feedback gain is 1 and 50.

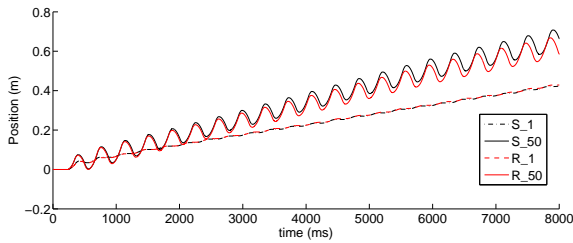


Fig. 12: Position of the end-effector in velocity control with/wihtout Reichardt-Model when feedback gain is 1 and 50.

In this experiment, due to mechanical restriction the differences of the control performances are not obvious when the feedback gain increases. As the length of the linear axis is limited, it is not allowed to observe the control performance in steady state. Besides, in order to protect the linear axis an output saturation module is added in the experiment. Therefore, the unstable control performance is not possible to achieve. However, depends on the simulation results, the following conclusion can still be made: velocity control with Reichardt-Model in its feedback is more stable than the one without Reichardt-Model.

Experiment2: In next two experiments, a resolution of 1280×480 pixels is chosen. The camera runs at framerate of 500fps. When the a high framerate is selected, the captured image is dark due to the short exposure time and is difficult for image processing. Therefore, a LED is mounted in front of the camera as the target object in the experiment.

The image processing is running to find the features in the image plane. In the experiment, there is only one LED mounted. Thus it is supposed to be only one feature that can be found in the image. The image processing is started by the threshold, through which the pixels with high illuminance are

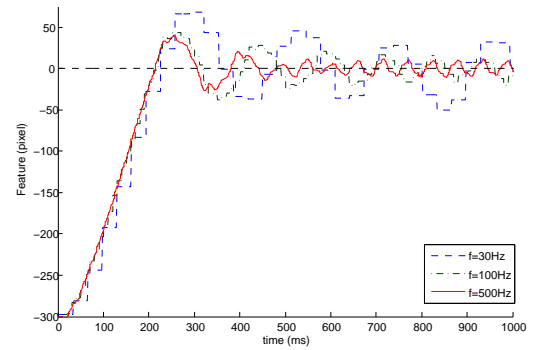


Fig. 13: Feature error trajectory when $K_p = 2.5 \times 10^{-4} N \cdot /pixels^2$ with different sampling time.

found. Then the resulted binary image is passed to a function that finds the contour of the selected pixels. Finally, the centroid is computed. The summed image processing time is about $1.5ms$ which is short enough for a vision system running at a frequency of 500Hz.

The coordinates of the centroid is transferred to the PC on which the control model runs. Since the linear axis has only 1-DOF, only x coordinate is utilized in the control. Then the image feature error between the desired feature and current feature is computed and the controller gives out the torque which moves the slide such that the error decreases. In the experiment, the desired feature point is set to $\xi = 670$ pixels, and the initial feature point is $\xi(0) = 970$ pixels. Thus the initial feature error is $\xi(0) = -300$ pixels. The fixed overall time-delay is about 5ms when no additional time-delay unit is present.

The control output is given by:

$$\tau = \frac{\alpha\lambda}{Z} K_p \ddot{\xi} - K_v \dot{q} \quad (5)$$

where $Z = 1m$, $K_p = 2.5 \times 10^{-4} N \cdot m / pixels^2$, $K_v = 2N \cdot m \cdot s / deg$. \dot{q} could be obtained either from the Reichardt-Model or by differentiating the output of the position sensor (in this experiment: \dot{q} is got from position sensor).

The results of the first experiment are shown in Fig.13. Vertical axis represents the feature error ξ in the image plane (expressed in pixels), while the horizontal axis is the time. The visual feedback of three different sampling rate (30Hz, 100Hz, 500Hz) is tested. As shown in Fig.13, after the transient the three feature error trajectories tend asymptotically to a small neighborhood of zero. The feature error oscillates around zero instead of settling down as time increases. The visual feedback of 30Hz has a oscillate amplitude of about 50pixels, while the 100Hz visual feedback oscillates at a amplitude of 20pixels. The 500Hz visual feedback has the smallest amplitude, 12pixels, which means a relatively better performance.

Experiment3: In this experiment, the system is tested with different time-delay when the visual feedback has a high sampling rate of 500Hz. Since several parts of the overall time-delay are fixed: exposure time, time for data distribution, and time for mechanical motion of the linear

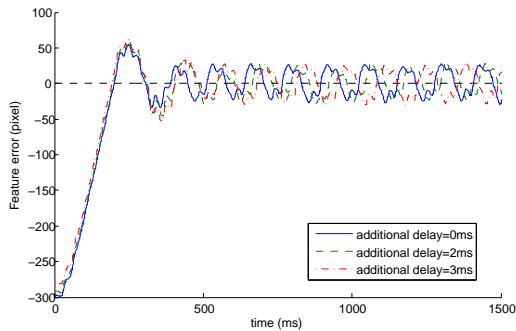


Fig. 14: Feature error trajectory when $K_p = 2.5 \times 10^{-4} N \cdot m/pixel^2$ with different additional time-delay, sampling rate is 500Hz.

axis, an easy way to tune the time delay is to add an artificial time-delay before sending data to the controller. Different additional time-delay is tried: 0ms, 2ms, 3ms. Fig.14 shows the experimental results. It is a little difficult to tell the difference between these systems from Fig.14. Thus the variance and integrated feature error in the time interval [0.5 1.5]s are calculated:

Additional delay (ms)	Variance (pixel ²)	Integrated error (pixel)
0	288.7	15790.8
2	331.6	16849.9
3	756.3	25300.9

TABLE I: Result Analysis

Table 1 indicates that, the system with less time-delay has better performance (smaller variance and smaller integrated error). Therefore, in the system design time-delay should be taken into consideration.

VI. CONCLUSIONS

In this paper, the biologically inspired motion detector Reichardt-Model is introduced into visual servo control. Because of the intrinsic properties of the Reichardt-Model, the control system with time-delay in its feedback loop is demonstrated to be stable. As the first step of the study, an high-speed IBVS with up to 500Hz has been built up in the lab. The simulation results demonstrate that the intrinsic properties of Reichardt-Model prevent the control system from getting unstable when feedback gain gets relative high and time-delay is presented. Besides, the experimental results demonstrated that, the system with visual feedback of higher sampling time takes less time to tend asymptotically to zeros and also has smaller amplitude when it oscillates around zero. Moreover, less time-delay brings the system to a better performance.

In the future, real-time visual servo control with Reichardt-Model in its inner velocity control loop will be built up. The comparison of the control performance of the visual system with and without Reichardt-Model will be carried out. To realize high-speed and real-time control, the implementation

of the Reichardt-Model on an FPGA platform and its integration into visual servo control will also be considered.

VII. ACKNOWLEDGMENTS

This work is supported in part within the DFG excellence initiative research cluster *Cognition for Technical Systems – CoTeSys*, see also www.cotesys.org and the Bernstein Center for Computational Neuroscience Munich, see also www.bccn-munich.de.

REFERENCES

- [1] S. Hutshison, G.D. Hager, and P. I. Corke, "A tutorial on visual servo control," *IEEE Transactions on Robotics and Automation*, vol. 12, pp. 651–670, 1996.
- [2] T. Senoo, A. Namiki, and M. Ishikawa, "Ball control in high-speed batting motion using hybrid trajectory generator," *International Conference on Robotics and Automation*, pp. 1762–1767, 2006.
- [3] N. Furukawa, A. Namiki, S. Taku, and M. Ishikawa, "Dynamic regrasping using a high-speed multifingered hand and a high-speed vision system," *International Conference on Robotics and Automation*, pp. 181–187, 2006.
- [4] J.A. Gangloff, M.F. de Mathelin, and S. Univ. Louis Pasteur, "High speed visual servoing of a 6 dof manipulator using mimopredictive control," *Robotics and Automation*, vol. 4, pp. 3751–3756, 2000.
- [5] Y. Nakabo, M. Ishikawa, H. Toyoda, and S. Mizuno, "1ms column parallel vision system and its applications of highspeed target tracking," *International Conference on Robotics and Automation*, vol. 1, pp. 650–655, 2000.
- [6] A. Borst and J. Haag, "Neural networks in the cockpit of the fly," *Journal of Comparative Physiology A*, vol. 188, pp. 419–437, 2002.
- [7] B. Hassenstein and W. Reichardt, "Systemtheoretische Analyse der Zeit-Reihenfolgen, und Vorzeichenauswertung bei der Bewegungsperzeption des Ruesselkaefers," *Naturforsch.*, vol. 11b, p. 1956, 1956.
- [8] H. Krapp and R. Hengstenberg, "A fast stimulus procedure to determine local receptive field properties of motion-sensitive visual interneurons," *Vision Research*, vol. 37, pp. 225–234, 1997.
- [9] T. Neumann and H. Bulthoff, "Insect inspired visual control of translatory flight," *Advances in Artificial Life. 6th European Conference, ECAL 2001. Proceedings*, vol. 2159, pp. 627–636, 2001.
- [10] C. M. Higgins and S. A. Shams, "A biologically inspired modular vlsi system for visual measurement of self-motion," *IEEE SENSORS JOURNAL*, vol. 2, pp. 508–528, 2002.
- [11] A. Warzecha and M. Egelhaaf, "Intrinsic properties of biological motion detectors prevent the optomotor control system from getting unstable," *The Royal Society*, vol. 351, pp. 1579–1791, 1996.
- [12] T.G. Zhang, H.Y. Wu, A. Borst, K. Kuehnlitz, and M. Buss, "An fpga implementation of insect-inspired motion detector for high-speed vision systems," *IEEE International Conference on Robotics and Automation (ICRA)*, pp. 335–340, 2008.
- [13] E. Malis, "Survey of vision-based robot control," *European Naval Ship Design, Captain Computer IV Forum*, April 2002.
- [14] E. Malis, F. Chaumette, and S. Boudet, "Positioning a coarse-calibrated camera with respect to an unknown planar object by 2d 1/2 visual servoing," in *Proc. 5th IFAC Symposium on Robot Control*, vol. 2, Nantes, France, 1997, pp. 517–523.
- [15] R. Mahony, P. Corke, and T. Hamel, "Dynamic image-based visual servo control using centroid and optical flow features," *Dynamic Systems, Measurement, and Control*, vol. 130, pp. 1–11, 2008.
- [16] A. Crual and F. Chaumette, "Positionning a camera parallel to a plane using dynamic visual servoing," *Conf. on Intelligent Robotics and Systems*, vol. 1, pp. 43–48, 1997.
- [17] B. Espiau, "Effect of camera calibration errors on visual servoing in robotics," *3rd International Symposium on Experimental Robotics*, October 1993.
- [18] L.E. Weiss, A.C. Sanderson, and C.P. Neuman, "Dynamic sensor-based control of robots with visual feedback," *IEEE J. Robot. Automat.*, vol. 3, pp. 404–417, 1987.
- [19] R. Kelly, R. Carelli, O. Nasisi, B. Kuchen, and F. Reyes, "A stable visual servo controller for camera-in-hand robotic systems," *International Conference on Advanced Robotics*, pp. 117–123, 1997.
- [20] *Manual of "Models STB2504-2510"*. [Http://www.copleycontrols.com/](http://www.copleycontrols.com/).